Molecular inclusion of organometallic sandwich complexes within hybrid cavitand-resorcin[4]arene receptors†

Maria Angeles Sarmentero[a] and Pablo Ballester*[a,b]

Received 17th May 2007, Accepted 1st August 2007
First published as an Advance Article on the web 14th August 2007
DOI: 10.1039/b707442e

Two different hybrid cavitand-resorcin[4]arenes are shown to be effective and selective receptors for the molecular inclusion of positively charged organometallic sandwich complexes of appropriate size. The binding constants of the 1 : 1 complexes formed with a series of neutral and positively charged metallocenes have been calculated using different titration techniques. The motion of the included metallocene and the kinetics of the complexation process are investigated. The voltammetric behaviour of the inclusion complexes formed with cobaltocenium is also studied.

Introduction

The confinement of guests within molecular vessels modifies their chemical behaviour. On the one hand, included guests can undergo reactions with significant rate enhancement and improved product selectivity.[1] On the other hand, the inclusion of redox-active guests, generally, tends to slow down the kinetics of heterogeneous electron transfer reactions and shifts the half-wave redox potential.[2] Several inclusion complexes containing electroactive metallocenes as guests have been reported.[3] Cyclodextrins tend to include preferentially neutral organometallic sandwich complexes in their internal hydrophobic cavities due to hydrophobic interactions.[4] Cucurbit[7]uril forms 1 : 1 inclusion complexes with cobaltocenium **1a**$^+$ and ferrocenium **1b**$^+$ by a combination of hydrophobic and ion-dipole interactions.[5] In non aqueous solvents, however, and to the best of our knowledge the inclusion of cobaltocenium cation **1a**$^+$ has only been achieved using supramolecular dimeric[6] and hexameric[7] capsules mainly through cation–π interactions. Nevertheless, hexameric and even dimeric capsules are harder to characterize or manipulate in solution than individual host molecules.

Recently, we described that hybrid cavitand-resorcin[4]arene **2a** formed a thermodynamically and kinetically stable 1 : 1 complex with tetraethylammonium cation **3**$^+$ (Fig. 1).‡ The **3**$^+$@**2a** complex is stabilized by cation–π and CH–π interactions with an association constant value of $1.4 \pm 0.4 \times 10^5$ M^{-1} in methanol.[8] We also found examples in the literature describing the similarity in the binding affinity of the cobaltocenium cation **1a**$^+$ with that of the tetraethylammnonium cation **3**$^+$ towards the inner cavity of a dimeric capsule formed by tetraurea calix[4]arene[6] or the tetrahedral cluster cavity of the supramolecular coordination assemblies

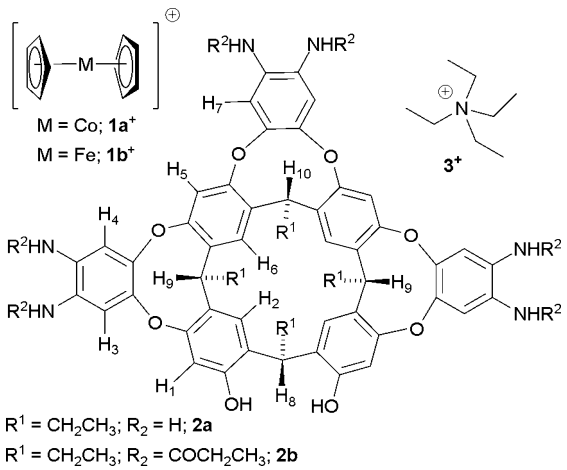

Fig. 1 Molecular structures of receptors **2a** and **2b**, cationic sandwich complexes **1a**$^+$, **1b**$^+$ and tetraethylammonium cation **3**$^+$.

of M_4L_6 stoichiometry.[9] In fact, the calculated volume inside the van der Waals surface of cobaltocenium **1a**$^+$ (135 Å^3) and its overall dimensions closely resemble those of the tetraethylammonium cation **3**$^+$ (156 Å^3).[10] In addition, both species are monocationic and prone to be engaged in cation–π and CH–π interactions. We decided to undertake this work to evaluate the efficiency of the neutral hybrid cavitand-resorcin[4]arene hosts **2** in the molecular inclusion of organometallic sandwich complexes.

The three diaminobenzene groups of **2** constitute the cavitand portion of the receptor. These groups can adopt an axial or an equatorial conformation. When the three groups are axial, the receptor contains an enforced scoop-shaped cavity having a wider open-end than that encountered in the native cavitands derived of resorcin[4]arenes.[11] Accordingly, we believe that these hosts may be more suitable molecular receptors for the pursuit of organometallic chemistry capable of proceeding with an included metal center.

Binding of organometallic sandwich complexes

The complexation of **2a** with cobaltocenium **1a**$^+$·PF_6^- was first probed using ^{1}H NMR titration techniques. The ^{1}H NMR spectrum of **2a** in MeOH-d_4 shows broad signals for all the

[a]*Institute of Chemical Research of Catalonia (ICIQ), Avda. Països Catalans 16, 43007 Tarragona, Spain. E-mail: pballester@iciq.es; Fax: +34 977 920221; Tel: +34 977 920206*
[b]*ICREA, Pg. Lluís Companys 23, 08010 Barcelona, Spain. E-mail: pau.ballester@icrea.es*

† Electronic supplementary information (ESI) available: Curve fitting of the titrations and additional electrochemical and spectroscopic data. See DOI: 10.1039/b707442e

‡ We refer to receptor **2** as a hybrid cavitand-resorcin[4]arene since only six of the eight hydroxyl groups of the native resorcin[4]arene skeleton have been used to elaborate its intrinsic cavity.

aromatic protons as well as for the methine protons H_9 and H_{10} (Fig. 2). This is probably due to dynamic effects involving exchange equilibration between different conformations of **2a**. The addition of 0.3 equivalents of **1a**$^+$·PF_6^- to a 5.09 mM solution of **2a** in MeOH-d_4 modifies the aromatic and methine signals. Particularly, the signal assigned to the methine protons H_8 broadens. Also, a new singlet assigned to the protons of complexed **1a**$^+$ can be observed at $\delta = 3.75$ ppm. When one equivalent of **1a**$^+$ is present in solution, all signals of **2a** are sharp and well resolved while the signal at $\delta = 3.75$ ppm is significantly broader.

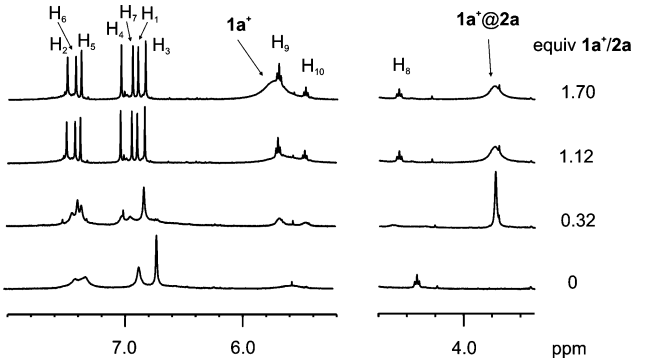

Fig. 2 Changes in two regions of the ^{1}H NMR spectra acquired at 298 K during the titration of **2a** with **1a**$^+$·PF_6^- in MeOH-d_4. [**2a**] = 5.09 mM. See Fig. 1 for proton assignments of **2a**.

The addition of an excess of metallocene **1a**$^+$ has a negligible effect on the proton signals of **2a**. At 1.7 equivalents of **1a**$^+$ a new broad signal centered at $\delta = 5.65$ ppm becomes evident. This is the chemical shift for the signal of the protons of free **1a**$^+$. Taken together, these observations indicate that hexaamine **2a** and metallocene **1a**$^+$ form, in MeOH-d_4, a complex with 1 : 1 stoichiometry having a stability constant too high to be measured accurately using this technique. Furthermore, the complexation process restricts the conformation flexibility of free **2a** to the vase conformer.

The aromatic cavity of the vase conformer of **2a** is electronically rich and capable of including cobaltocenium **1a**$^+$ (Fig. 3) by offering complementary cation–π, CH–π and π–π interactions. The magnetic microenvironment within the seven aromatic rings of **2a** cause a large upfield shift of the protons of **1a**$^+$ ($\Delta\delta = -1.9$ ppm). The observation of two different but broad proton signals for free and bound **1a**$^+$ indicates that the complex **1a@2a** has a moderate kinetic stability on the ^{1}H NMR timescale. The fact that the incremental addition of **1a**$^+$ induces a rapid broadening of the signal for included cobaltocenium hints to a second order process for the guest exchange.

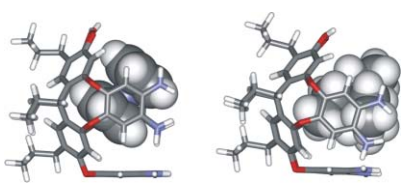

Fig. 3 CAChe minimized structures of cobaltocenium **1a**$^+$ (left) and tetraethylammonium cation **3**$^+$ (right) included in the scoop shaped cavity of **2a**. **1a**$^+$ and **3**$^+$ are shown with van der Waals radii to highlight the similarity of dimensions.

The binding affinity of receptor **2a** for cobaltocenium **1a**$^+$ in methanol was first established by means of a competitive displacement assay, using pyrene modified *N*-methylpyridinium cation **6**$^+$ as fluorescent indicator (Fig. 4).[12] The addition of **2a** to a MeOH solution of **6**$^+$ results in an efficient fluorescence quenching (up to 96%, $\lambda_{exc} = 430$ nm, $\lambda_{em} = 580$ nm). The association constant for the **6**$^+$**@2a** complex was calculated as $K_a = 1 \pm 0.2 \times 10^4$ M^{-1} from the observed linear relationship dependence of I_0/I on [**6**$^+$].[13] Successive addition of cobaltocenium **1a**$^+$ to the complex formed in the presence of **2a** (1.5×10^{-4} M) and **6**$^+$ (4.2×10^{-4} M) led to the fluorescence recovery of **6**$^+$ reaching a plateau at high concentrations of cobaltocenium. The binding constant for **1a**$^+$**@2a** was calculated as $K_a = 2.20 \pm 0.7 \times 10^5$ M^{-1}.

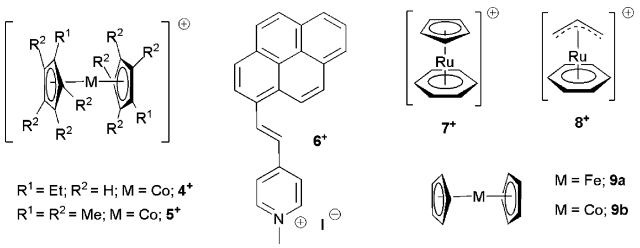

Fig. 4 Molecular structures of some guests used in this study.

Isothermal titration calorimetry (ITC) is an alternative technique to spectroscopic titration and recently has attracted considerable attention for the study of binding processes in solution.[14] ITC measurements allow the direct determination of the association constant, K_a, and the binding enthalpy, $\Delta H°$, providing a complete thermodynamic picture of the interaction under investigation. Calorimetric titrations were performed by the sequential injection of a methanol solution of cobaltocenium **1a**$^+$ ([**1a**$^+$] = 2.44 mM) to a methanol solution containing the hexaamine receptor **2a** ([**2a**] = 0.20 mM). The top graph in Fig. 5 shows raw data of the ITC experiment in terms of μcal per second plotted against time in minutes, after the integration baseline has been subtracted. The bottom graph shows normalized integration data of the heat (exothermic) evolved per injection in terms of kcal mol^{-1} of injectant (**1a**$^+$) plotted against the molar ratio **1a**$^+$–**2a**. The binding isotherm is sigmoidal and shows an inflection point at a molar ratio of approximately 0.83, indicating a 1 : 1 stoichiometry for the complex being formed (**1a**$^+$**@2a**). The heat of the binding was fitted using the Microcal ITC Data Analysis module to a 1 : 1 binding algorithm (red line) to give a binding constant of $K_a = 141 \pm 10 \times 10^3$ M^{-1}. Formation of the **1a**$^+$**@2a** complex is strongly enthalpy driven ($\Delta H = -10.5 \pm 0.1$ kcal mol^{-1}). The observed negative enthalpy change occurs from the formation of several favourable cation–π and CH–π interactions. The small adverse negative entropy ($T\Delta S = -3.5$ kcal mol^{-1}) probably arises from the difference in the loss of translational and conformational entropy on complex formation and the gain in entropy experienced by solvent molecules released to the bulk during the complexation process. The two association constant values determined for the **1a**$^+$**@2a** complex using two different techniques are in good agreement within experimental error. The high stability constant of the complex in MeOH (>10^5 M^{-1}) indicates good complementarity between the receptor **2a** and sandwich metallocene **1a**$^+$.

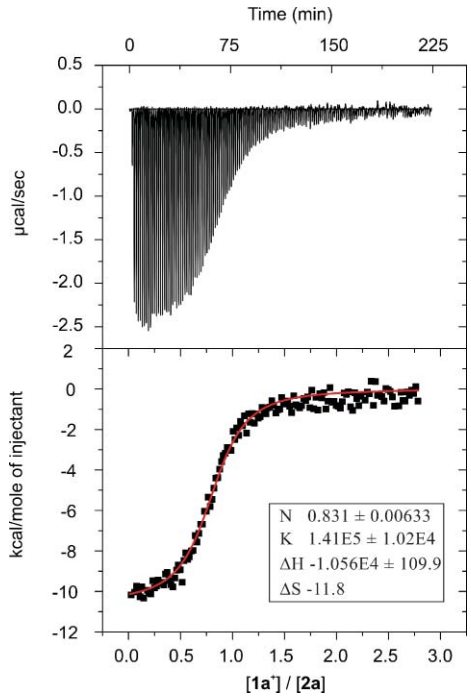

Fig. 5 ITC titration experiment of the formation of the **1a**$^+$@**2a** complex. Top: raw data. Bottom: normalized integration data of the evolved heat per injection in terms of kcal mol^{-1} of injectant (**1a**$^+$) plotted against the molar ratio **1a**$^+$–**2a**. To determine the values of the thermodynamic variables (ΔH, ΔG and ΔS) the ITC data have been fitted to a 1 : 1 binding model (red line).

The monosubstitution at both cyclopentadienyl rings with one ethyl group, as in derivative **4**$^+$, reduces considerably the binding affinity with **2a**. The stability constant of the **4**$^+$@**2a** complex was also measured using two different techniques and the calculated values (Table 1) indicate a drop of two orders of magnitude compared to that of the **1a**$^+$@**2a** complex. Bis(pentamethylcyclopentadienyl)cobalt(III) **5**$^+$ and neutral bis(cyclopentadienyl)iron(II) **9a** are not bound by **2a**. The lack of affinity of **2a** for metallocene **5**$^+$ is probably caused by a mismatch in size. However, the affinity loss in the case of **9a**, which is roughly the same size as **1a**$^+$ but differs in its positive charge, is due to the absence of cation–π interactions that only operate between **1a**$^+$ and the aromatic rings of the hexaamine receptor **2a**. Therefore, we conclude that receptor **2a** features a remarkable size and charge selectivity in the molecular inclusion of stable organometallic sandwich complexes.

We wanted to explore the binding properties of **2a** with ruthenium sandwich complexes **7**$^+$ and **8**$^+$, however, the unexpected low stability of these complexes in the presence of **2a** forced us to consider the hexaamide derivative **2b** as an alternative receptor.§ Receptor **2b** is not soluble in MeOH so the study of its binding properties with organometallic sandwich complexes was performed in acetone.

Fig. 6 shows the ^{1}H NMR titration of **2b** with metallocene **1a**$^+$. The proton signals of **2b** in acetone-d_6 are sharp and well resolved. The presence of two well defined triplets at $\delta = 5.63$ and 5.74 ppm

§ The polyamine character of **2a** may induce competitive complexation with the metal center.

Table 1 Binding constants of cationic metallocene sandwich complexes with receptors **2**

	Receptor **2a**	Receptor **2b**
Metallocene	$K_a/10^3$ M^{-1} [a]	$K_a/10^3$ M^{-1} [b]
1a$^+$·PF_6^-	220 ± 70[c]/141 ± 20[d]	4.0 ± 0.4[d]/4.0 ± 0.6[e]
4$^+$·PF_6^-	2.4 ± 0.5[d]/3.4 ± 0.3[e]	0.17 ± 0.02[e]
5$^+$·PF_6^-	<0.01	<0.01
6$^+$·I^-	10 ± 2	
7$^+$		0.23 ± 0.07[e]
8$^+$		0.14 ± 0.02[e]
9a	<0.01	<0.1
9b	0.020[e]	0.106[e]

[a] Determined in MeOH. [b] Determined in acetone. [c] Fluorescence competitive assay. [d] ITC titration. [e] ^{1}H NMR titration. [f] CV data.

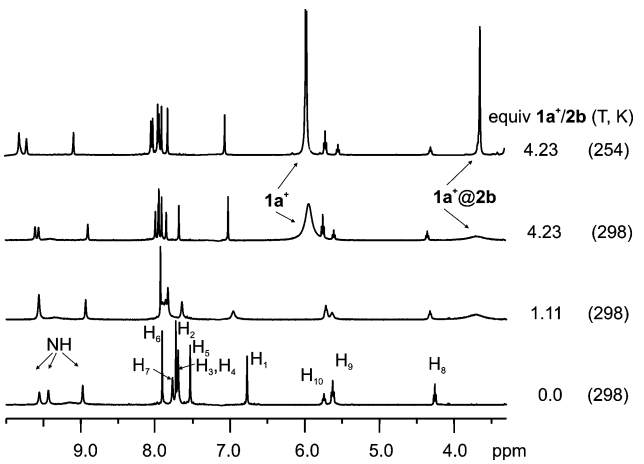

Fig. 6 Changes in one region of the ^{1}H NMR spectra acquired at 298 K during the titration of **2b** with **1a**$^+$·PF_6^- in acetone-d_6. Top spectrum: low temperature (254 K) ^{1}H NMR spectrum of solution of **2b** containing 4.23 equiv. of **1a**$^+$. [**2b**] = 3.94 mM. See Fig 1 for proton assignments of **2b**.

for the methine protons H_9 and H_{10} are indicative that **2b** exists in a vase-like conformation in acetone-d_6, probably stabilized by the intramolecular hydrogen bonds that stitch the upper rim of the receptor when the aromatic walls adopt the "axial" orientation. The incomplete head-to-tail seam of intramolecular hydrogen bonds formed by the six secondary amides of **2b** results in two cycloenantiomers, with clockwise or counterclockwise orientation (Fig. 7).[15]

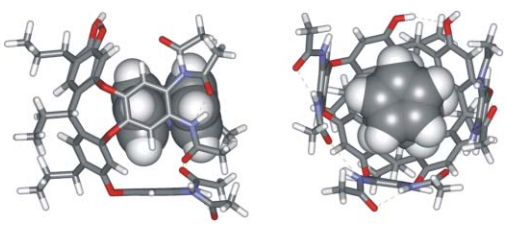

Fig. 7 Side view and top view of a CAChe minimized structure for the **1a**$^+$@**2b** complex having counterclockwise arrangement of the intramolecular hydrogen bonds of the amides.

The ^{1}H NMR spectra of **2b** in acetone-d_6 showed only three different downfield shifted NH singlet and seven aromatic proton

signals indicating that the interconversion between two enantiomers is fast on the NMR timescale (Fig. 6, bottom spectrum).

Addition of incremental amounts of **1a**$^+$ to a 3.94 mM solution of **2b** produces broadening and chemical shift changes of the aromatic signals, as well as the methine triplets. A broad signal corresponding to included **1a**$^+$ emerges at $\delta = 3.78$ ppm, an identical value to that observed in the case of **2a** ($\delta = 3.75$ ppm) demonstrating that **1a**$^+$ experiences a similar shielding microenvironment in both receptors. After the addition of more than one equivalent of **1a**$^+$ the proton signals for **2b** sharpen again and a broad signal for free **1a**$^+$ can be observed at $\delta = 5.93$ pm. All the association constants for receptor **2b** with the series of sandwich complexes were calculated using ^{1}H NMR titrations. Consistently, the NH signal of the free receptor **2b** at $\delta = 9.57$ pm shifted upfield upon addition of the metallocene while the H_1 aromatic signal at $\delta = 6.67$ pm experienced a downfield shift. The titration data obtained for the chemical shift change of the proton signals resonating at $\delta = 5.63$ and 6.67 ppm for free **2b** were fitted to a 1 : 1 binding model, and the calculated association constants shown in Table 1 are averaged values. The binding affinities are at least one order of magnitude smaller than those observed for **2a** in MeOH, but the size and charge selectivity observed in the inclusion of the metallocenes is completely retained by **2b**. The ruthenium complexes **7**$^+$ and **8**$^+$ are included with similar affinities, which are also comparable to that of **4**$^+$. Most likely, the gain in size produced by the substitution of one C_5H_5 ligand by C_6H_6 is responsible for the observed reduction in binding affinity for **7**$^+$. The loss of affinity of **2b** for **8**$^+$ can be attributed to a modification of some of the intermolecular interactions stabilizing the complex.

The thermodynamic analysis of the binding of cobaltocenium **1a**$^+$ with receptor **2b** in acetone was also undertaken using ITC. The ITC results show that the binding is moderately enthalpy-driven ($\Delta H = -2.4 \pm 0.02$ kcal mol^{-1}) with a strong favorable entropy term ($T\Delta S = 2.5$ kcal mol^{-1}). The entropic benefit is due to the release of ordered acetone molecules from the surface of the free species upon formation of the complex that causes a net increase in disorder for the overall process (desolvation + binding). The weak enthalpic gain of binding is probably due to the fact that the relatively electron-rich aromatic walls of the receptor are comparable matches for the bound cationic guest in terms of cation–π interactions that the acetone molecules solvating the free guest and establishing cation–dipole interactions with it.

The inclusion complexes formed with receptors **2** and the cationic cobalt(III) metallocenes **1a**$^+$ and **4**$^+$ can be easily detected by mass spectrometry. When solutions of receptors **2** containing an excess of the cation are ionized with an electrospray ionization source, intense signals corresponding to singly charged [**1**@**2**]$^+$ and [**4**@**2**]$^+$ complexes can be observed. This result confirms the 1 : 1 stoichiometry assigned to these complexes.

The relative binding affinity of **2** toward the two metallocenes was also established by ESI-MS competitive binding experiments. In these experiments, the receptor **2** at fixed concentration was mixed with equimolecular amounts of the two metallocenes **1a**$^+$ and **4**$^+$ and the corresponding positive ESI-MS spectra were measured (Fig. 8). These experiments allow the easy determination of which of the two metallocenes in the mixture is preferentially bound by the receptor **2**. In both cases, intense signals for both 1 : 1 complexes are observed with apparent preference for **1a**$^+$@**2** over

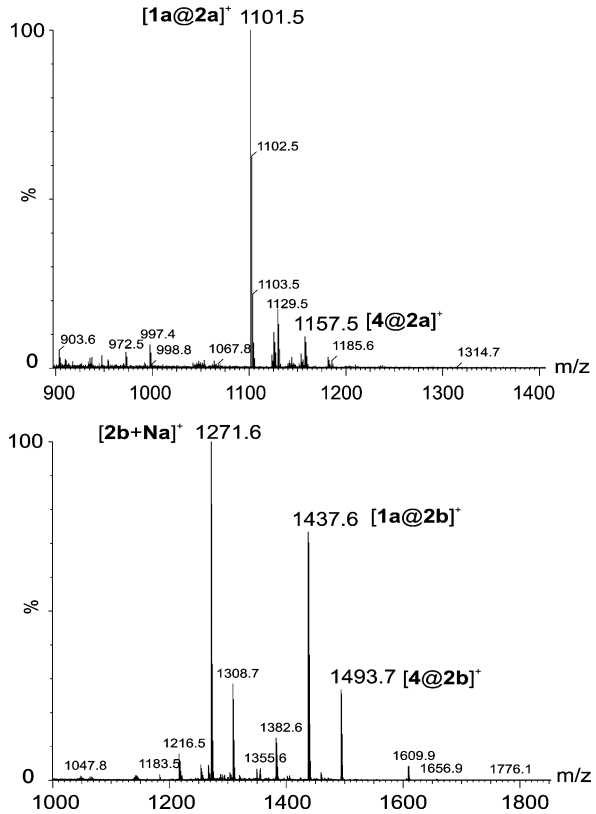

Fig. 8 ESI-MS spectra of the competitive experiments of **2a** (above) and **2b** (below) with cations **1a**$^+$ and **4**$^+$.

4$^+$@**2**, a result in complete agreement with the binding experiments performed in solution.

Motion of the metallocene inside the cavity and kinetics of guest exchange

Several favourable binding geometries for the **1a**$^+$@**2b** complex can be modelled when the binding characteristics of the aromatic cavity of **2b** are combined with the geometric requirements of the binding forces involved in the complexation of cobaltocenium **1a**$^+$, mainly cation–π, CH–π and π–π interactions. In order to explore the experimental observation of different complex geometries during the inclusion of **1a**$^+$ by **2b**, we carried out a variable temperature ^{1}H NMR study on the titration sample containing 4.23 equivalents of cobaltocenium **1a**$^+$.

On cooling the above solution to 254 K, the guest exchange of (excess) free and included **1a**$^+$ becomes very slow with respect to the NMR timescale as evidenced by the sharpening of the proton signal of free **1a**$^+$ (Fig. 6, top spectrum). Furthermore, the simultaneous observation of a unique and very sharp singlet ($\delta = 3.75$ ppm) for the included **1a**$^+$ indicates that all hydrogen resonances of included **1a**$^+$ are chemically equivalent. On the one hand, this result demonstrates that the broadening of the proton signals for free and included **1a**$^+$ observed at r.t. is just due to the in–out guest exchange. On the other hand, it also shows that the included **1a**$^+$ *tumbles and spins freely within* **2b** and can easily interconvert between different binding geometries. Lowering the temperature to 200 K has no further effect on the signals of free and bound **1a**$^+$. At this temperature, however, the guest in–out

exchange process is too slow to be detected through an EXSY experiment but the motion of **1a**$^+$ inside the cavity remains very fast. The flexibility of the hybrid-cavitand maintained in the vase conformation by weak hydrogen bonds that can be easily stretched and its wide open-end facilitates the motion of the included guest.

We also performed a 2D EXSY experiment at 298 K to determine the rate of self-exchange of the guest.[16] We calculated an exchange rate constant $k_{out} = 6.02\ s^{-1}$ corresponding to a chemical exchange barrier, $\Delta G^{\neq 298\ K}_{diss}$, for guest exiting the host of 16.38 kcal mol^{-1}.[17] Previous publications have shown that the barrier to unfolding a deep cavitand without hydrogen bonding stabilization is 10–11 kcal mol^{-1},[18] while the barrier for unfolding a related native cavitand with eight intramolecular hydrogen bonds instead of five is 17 kcal mol^{-1}.[19] The barrier of self-exchange depends not only on the energy required to reorganize the host to the conformation that can release the guest but also upon the nature of the guest, which in turn, is responsible for the thermodynamic stability of the complex. The free energy for the formation of the **1a**$^+$@**2b** complex is $\Delta G_{\mathbf{1a}^+@\mathbf{2b}} = -4.9$ kcal mol^{-1}. Accordingly, we can estimate the barrier to reorganize the host during the dissociation of the hybrid-cavitand complex having a vase conformation stabilized by five intramolecular hydrogen bonds as $\Delta G^{\neq 298\ K}_{conformation} = \Delta G^{\neq 298\ K}_{diss} + \Delta G^{298\ K}_{\mathbf{1a}^+@\mathbf{2b}} = 11.48$ kcal mol^{-1}. The estimated value for the conformational change is very close to the barrier for unfolding a deep cavitand. Taken together, these findings indicate that the exchange of the guest requires the unfolding of the cavitand[19] and that the five intramolecular hydrogen bonds present in **2b** produce a moderate increase of the unfolding barrier compared to a deep cavitand deprived from such type of stabilization. The high barrier for guest exchange calculated for **2b**, in which one of the aromatic walls of the native cavitand structure is removed, hints to a general exchange mechanism for cavitands requiring the opening of more than one "flap" of the cavity. Diederich *et al.* have recently shown exchange in cavitands possibly *via* opening of two opposite walls.[20]¶

The guest exchange for the inclusion of 1,1′-diethylcobaltocenium **4**$^+$ within the cavity of receptor **2b** turns out to be moderate on the ^{1}H NMR timescale at 298 K giving rise to a broad signal centered at $\delta = 5.60$ ppm and corresponding to the average of the cyclopentadienyl proton signals of free and included **4**$^+$ (Fig. 9). This result comes as no surprise since the stability constant of the **4**$^+$@**2b** complex, one of the factors controlling the dissociation barrier, drops more that one order of magnitude (~2 kcal mol^{-1}) compared to **1a**$^+$@**2b**. However, cooling at 203 K an acetone-d_6 solution containing **2a** ([**2a**] = 2.79 mM) and 2.4 equivalents of **4**$^+$ allowed the observation of two sets of proton signals corresponding to free and included **4**$^+$. At this temperature the cyclopentadienyl protons of the free metallocene **4**$^+$ appear as two broad singlets at $\delta = 5.86$ and 5.84 ppm respectively. The protons of included **4**$^+$ are identified by the presence of upfield ^{1}H NMR resonances due to the anisotropic magnetic shielding properties of **2b**. The cyclopentadienyl protons resonate at $\delta = 4.01$ and 3.55 ppm and a very broad signal is observed at $\delta = -0.07$ ppm corresponding to the methyl group of included **4**$^+$ (*vide infra*).

¶ A dissociative exchange process that produces a vacuum in the cavity should have a prohibitive free energy barrier.

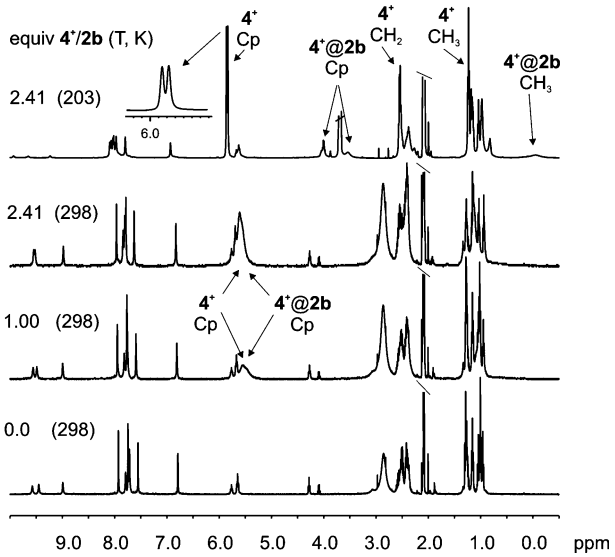

Fig. 9 Changes in the ^{1}H NMR spectra acquired at 298 K during the titration of **2b** with **4**$^+$·PF_6^- in acetone-d_6. Top spectrum: low temperature (203 K) ^{1}H NMR spectrum of solution of **2b** containing 2.41 equiv. of **4**$^+$. [**2b**] = 2.79 mM.

The kinetic analysis of the complexation process of **4**$^+$ by **2b** was investigated by means of an EXSY experiment performed at 203 K (Fig. 10). At this temperature, the pseudo first order rate constant for complexation k_{in} is 1.23 s^{-1}, whereas the first order rate constant for decomplexation k_{out} is 3.19 s^{-1}. The activation free enthalpy for the dissociation, $\Delta G^{\neq 203\ K}_{diss}$, at 203 K is 11.26 kcal mol^{-1}. Clearly, decomplexation of included **4**$^+$ within **2b** occurs at a much faster rate than for **1a**$^+$. Probably, the reduced kinetic and thermodynamic stability of the **4**$^+$@**2b** complex is due to a shallower inclusion of the metallocene unit inside the cavity of the receptor. The two proton signals of the cobaltocenium moiety of **4**$^+$ experience a reduced effect of the shielding microenvironment

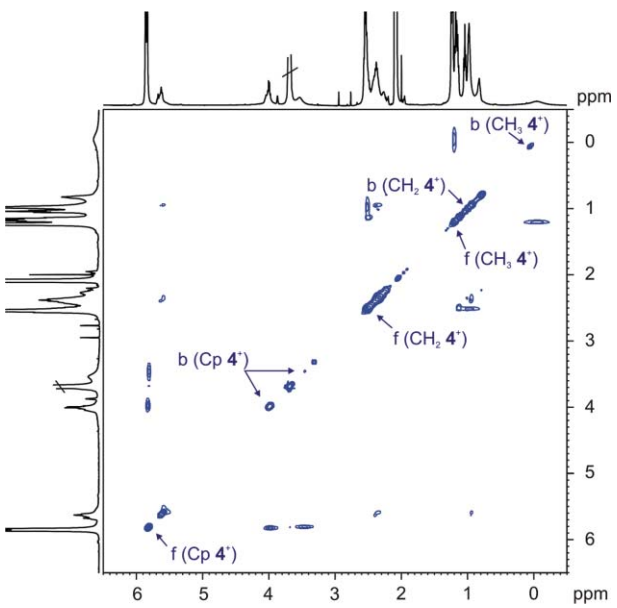

Fig. 10 ESXY ^{1}H NMR spectrum of **2b** ([**2b**] = 2.79 mM) containing 2.4 equivalents of **4**$^+$ in acetone-d_6 at 203 K (mixing time 0.3 s); b and f indicate bound and free signals.

of **2b** ($\Delta\delta = -1.0$ and -1.5 ppm) when compared to **1a**$^+$ ($\Delta\delta = -1.9$ ppm). Rebek *et al.* have already pointed out that the cavitands provide a gradient of magnetic anisotropy that shifts the residues bound deepest in the cavity the furthest upfield.[21] For **4**$^+$, it's one of the ethyl groups that is bound deepest in the cavity ($\Delta\delta(CH_2) \sim -1.6$ ppm and $\Delta\delta(CH_3) \sim -1.3$ ppm) moving the cobaltocenium moiety away from the end of the cavity. The number of signals observed for the included **4**$^+$, two signals for the cyclopentadienyl protons and just one signal for the methylene and the methyl protons of the ethyl group, can be explained if the guest tumbles fast on the NMR timescale inside **2b**. Consequently, all the chemical shifts observed for the included protons are a chemical shift average of at least two different magnetic environments (one deep in the cavity and another near the open end). The different broadening observed for the proton signals corresponding to free and bound **4**$^+$, easily noticeable in the signals of the ethyl group, demonstrate that while at 203 K the in–out exchange of the guest is slow on the ^{1}H NMR timescale, its motion inside the cavity occurs in a fast to moderate regime in the same timescale. The presence of the ethyl group on the metallocene reduces the rate of tumbling. Whereas **1a**$^+$ tumbles rapidly even at 200 K, **4**$^+$ shows slower tumbling and broad NMR signals at 203 K.

Voltammetric behavior of the inclusion complexes

We also investigated the voltammetric behaviour of complexes **1a**$^+$**@2a** and **1a**$^+$**@2b** in MeOH and acetone, respectively, and compared them with that of free **1a**$^+$. As shown in Fig. 11 the complexation of cobaltocenium **1a**$^+$ with **2a** can be easily detected by the observation of two redox couples during a cyclic voltammetry (CV) titration experiment.

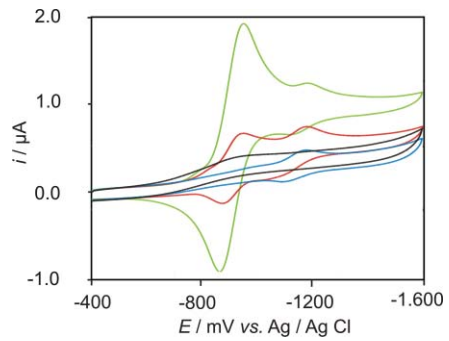

Fig. 11 Voltammetric response on glass carbon (0.071 cm^2) of: (a) 1.0 mM solution of **2a** also containing 0.1 M tetraoctylammonium bromide in the absence of any **1a**$^+$ (black) and in the presence of 0.5 equiv. (blue), 1.2 equiv. (red) and 3 equiv. (green) of **1a**$^+$.

The redox couple with a half-wave potential ($E_{1/2}$) at -911 mV comes from free **1a**$^+$ and the negatively shifted one at -1141 mV is from the inclusion complex **1a**$^+$**@2a**. We also detected a *ca.* 50% decrease in the peak current of the redox couple assigned to **1a**$^+$**@2a** when compared to that of free **1a**$^+$ at the same concentration. The shift of the new redox Co(II)/Co(III) couple for the included **1a**$^+$ toward cathodic values indicates that the oxidized, cationic form of Co(III), **1a**$^+$, is more strongly bound to the hybrid cavitand **2a** than neutral Co(II) **9b**. We suggest that the negative shift is caused by the thin layer of negative density present in the inner surface of **2a**, which generates a microenvironment that stabilizes included **1a**$^+$. The reduction in peak current of the redox couple assigned to the **1a**$^+$**@2a** complex is due to the slower diffusion of **1a**$^+$ when it is included.‖ The voltammetric behaviour of **1a**$^+$**@2b** is similar to that described above (see ESI†). The shift values in $E_{1/2}$ for **1a**$^+$ upon inclusion in **2** (-230 mv for **2a** and -93 mV for **2b**) were used to calculate the stability constant of the inclusion complexes with cobaltocene, **9b**. We obtained $K_{\mathbf{9b@2a}}/K_{\mathbf{1a^+@2a}} = 1.3 \times 10^{-4}$ and $K_{\mathbf{9b@2b}}/K_{\mathbf{1a^+@2b}} = 2.7 \times 10^{-2}$, which translates to $K_{\mathbf{9b@2a}} = 20\ M^{-1}$ and $K_{\mathbf{9b6@2b}} = 106\ M^{-1}$. The reduction of the guest eliminates the contribution of the cation–π interaction to the complex stabilities, which accounts for 5.3 kcal mol^{-1} in the case of **2a** and 2.1 kcal mol^{-1} for **2b**. This result can be ascribed to differences in the molecular electrostatic potential surface of the electron-rich cavities of **2**. Overall, we observe a remarkable selectivity in the binding of the positively charged guest **1a**$^+$, even using a neutral receptor. The CV results also demonstrate that the **1a**$^+$**@2** and **9b@2** complexes are kinetically stable enough to distinguish the included and free form of the redox active guest in the timescale of CV measurements. This also means that the electron transfer process proceeds in the included form. Clearly, the voltammetric data also support the inclusion of **1a**$^+$ within the aromatic cavity of receptors **2**.

Experimental

Computational procedures

Molecular modelling was performed using CAChe WorkSytem Pro Version 6.1.12.33. The structures of the complexes correspond to an energy minimum refined by performing an optimized geometry calculation in mechanics using augmented MM3 parameters as implemented in the software package.

General procedures

All reagents were obtained from commercial suppliers and used without further purification. All solvents were of HPLC grade quality, obtained commercially and used without further purification. Anhydrous solvents were collected from a solvent purification system SPS-400-6 from Innovative Technologies, Inc. Flash column chromatography was performed with Silica gel Scharlab60. ^{1}H and ^{13}C spectra were recorded on either a Bruker Avance DRX-400 or DRX-500 spectrometer with residual protio solvent as internal standard. ESI data were recorded on a Waters LCT Premier Electrospray TOF Mass Spectrometer. All guests, except **6**$^+$, **7**$^+$ and **8**$^+$, were obtained from Aldrich Chemical Company and were used as received. Guest **6**$^+$ was obtained as described in the literature.[22] Guests **7**$^+$ and **8**$^+$ were also prepared according to literature procedures.[23]

Synthesis of receptor 2a

In a flask were placed the hexanitro cavitand precursor[19b] (300 mg, 0.27 mmol), $SnCl_2$ dihydrate (2.10 g, 9.1 mmol) and a mixture of EtOH (30 mL) and concentrated HCl (6.5 mL). The mixture was heated at 70 °C overnight and the colour changed from orange to pale yellow. The solvent was partially evaporated and a white solid appeared, which was filtered to isolate the hydrochloride salt of **2a**

‖ $D_{red}(\mathbf{1a}^+) = 1.43 \times 10^{-6}$ cm^2 s^{-1}. $D_{red}(\mathbf{1a}^+\mathbf{@2a}) = 4 \times 10^{-7}$ cm^2 s^{-1}.

(70%). This solid was treated for 30 min with a two-layer mixture containing ethyl acetate and concentrated ammonia. The organic layer was separated, dried over Na_2SO_4, filtered and concentrated *in vacuo* yielding hexaamine **2a** as a pale yellow solid (80% yield). ^{1}H NMR (400 MHz, DMSO-d_6) δ 9.51 (br s, 2H), 7.68 (s, 2H), 7.54 (s, 2H), 7.13 (s, 2H), 6.76 (s, 2H), 6.69 (s, 2H), 6.55 (s, 2H), 6.48 (s, 2H), 5.4 (m, 3H), 4.42 (s, 4H), 4.31 (s, 8H), 4.00 (t, $J = 7.2$ Hz, 1H), 2.39–2.25 (m, 8H), 0.89 (t, $J = 7.2$ Hz, 3H), 0.83 (t, $J = 7.2$ Hz, 3H), 0.77 (t, $J = 7.2$ Hz, 3H). ^{13}C NMR (100 MHz, DMSO-d_6) 155.93, 155.60, 155.32, 152.33, 143.06, 142.95, 136.37, 135.24, 133.28, 133.21, 132.80, 130.09, 128.75, 125.27, 116.71, 109.86, 109.74, 109.43, 109.27, 36.32, 35.63, 35.44, 26.65, 25.97, 25.02, 13.05, 13.01, 12.97. HRMS *m/z* (MALDI) calcd for $C_{54}H_{53}N_6O_8$ $[M + H]^+$ 913.3925 found 913.3881.

Synthesis of receptor 2b

700 mg of the hexanitro cavitand precursor[19b] (0.63 mmol) and 3.0 g of $SnCl_2$ dihydrate (21.23 mmol) were suspended in a 4 : 1 mixture of EtOH and concentrated HCl (50 mL). The resulting suspension was heated at 70 °C overnight. The solution first turned orange and by the end of the reaction it was pale yelow. The EtOH was evaporated until a white residue was formed and only a couple of mls of liquid remained. A solution made with 8.5 g of K_2CO_3 in water (40 mL) and ethyl acetate (100 mL) was slowly added. Propionyl chloride (650 μL) was added and after 30 min another addition of propionyl chloride (650 μL) was carried out. The organic layer was separated and the suspension was extracted with ethyl acetate. The combined organic extracts were washed with brine, dried over Na_2SO_4, filtered and concentrated *in vacuo* to afford a white solid. This solid was taken up in a 1 : 1 mixture of toluene–EtOH (30 mL) and hydrazine (300 μL) was added. The mixture was heated to 70 °C for 1 h. Flash chromatography was performed on silica gel with the solvent mixture CH_2Cl_2–MeOH (100 : 2 → 100 : 3.5 → 100 : 5) to give hexaamide diol cavitand **2b** (60%). ^{1}H NMR (400 MHz, acetone-d_6) δ 9.68 (s, 2H), 9.55 (s, 2H), 9.02 (2H, s), 7.91 (s, 2H), 7.80 (s, 2H), 7.72 (s, 2H), 7.70 (s, 4H), 7.53 (s, 2H), 6.78 (s, 2H), 5.74 (t, $J = 8.3$ Hz, 1H), 5.62 (t, $J = 8.3$ Hz, 2H), 4.25 (t, $J = 8.3$ Hz, 1H), 2.62–2.43 (m, 12H), 2.43–2.28 (m, 8H), 1.28–1.22 (m, 12H), 1.12 (t, $J = 7.5$ Hz, 3H), 1.08 (t, $J = 7.5$ Hz, 3H), 1.01 (t, $J = 7.5$ Hz, 3H), 0.98 (t, $J = 7.5$ Hz, 6H), 0.93 (t, $J = 7.5$ Hz, 3H). ^{13}C NMR (100 MHz, acetone-d_6) 173.4 (C=O), 172.4 (C=O), 155.0, 154.6, 152.2, 149.6, 149.4, 148.9, 136.8, 135.9, 130.2, 129.1, 128.6, 127.8, 127.7, 126.8, 125.1, 124.5, 116.1, 109.2, 36.2, 35.8, 35.5, 30.3, 29.6, 29.5, 25.9, 25.1, 24.8, 12.1, 9.7, 9.6, 9.0. HRMS *m/z* (MALDI) calcd for $C_{72}H_{76}N_6O_{14}$ $[M + Na]^+$ 1271.5311 found 1271.5324.

Fluorescence titrations

Fluorescence experiments were conducted on an Aminco Bowman Series 2, at 298 K, in MeOH. The sample volume was 2 mL. The titration between hexaamine-diol **2a** and the ammonium salt $\mathbf{6}^+$ in MeOH was carried out by adding small aliquots of a solution of **2a** (3.3×10^{-4} M) to a MeOH solution of $\mathbf{6}^+$ (8.25×10^{-6} M). The concentration of the fluorescent indicator $\mathbf{2a}^+$ was kept constant throughout the titration. A spectrum was recorded after each addition and the resulting titration data were analysed using the SPECFIT computer program (1 : 1 binding model), as well as by means of a simple linear relationship ($I_0/I = 1 + K_a$ [$\mathbf{6}^+$]) ($K_a = 1 \pm 0.2 \times 10^4$ M^{-1}) derived by assuming that the fluorescence is completely quenched on complex formation. A similar value of binding constant was obtained using the two different mathematical treatments. The binding affinity of cobaltocenium cation $\mathbf{1a}^+$ to receptor **2a** in MeOH was established by means of a competitive displacement assay, using the pyrene modified *N*-methylpyridinium cation $\mathbf{6}^+$ as fluorescent indicator. The incremental addition of a solution of $\mathbf{1a}^+$ (0–0.35×10^{-3} M^{-1}) to the complex formed in the presence of **2a** (1.5×10^{-4} M) and $\mathbf{6}^+$ (4.2×10^{-4} M) led to the fluorescence recovery of $\mathbf{6}^+$ reaching a plateau at high concentrations of the cation. The binding constant for $\mathbf{1a}^+$@**2a** was calculated as $K_a = 2.20 \pm 0.7 \times 10^5$ M^{-1} by SPECFIT[24] analyses of the I/I_0 growth of fluorescence as a function of the added metallocene cation $\mathbf{1a}^+$ using a competitive binding scheme of two 1 : 1 complexes and only one fluorescence species, free $\mathbf{6}^+$.

^{1}H NMR titrations

All titrations were carried out on a Bruker 500 MHz spectrometer in MeOH-d_4 (**2a**) or acetone-d_6 (**2b**). The association constants were determined using 2.64–5.09 mM solutions of hexaamine-diol **2a** or hexaamide-diol **2b** in the appropriate solvent at 298 K, and adding aliquots of a solution of the corresponding salt, approximately 10 times more concentrated, in the same solvent. The receptor **2a–b** concentration was kept constant throughout the titration. The association constants between hexaamine **2a** and the cobaltocenium cations were determined by following the chemical change of the protons at 6.70 ppm (**2a**) or 5.63 and 6.67 ppm (**2b**) in the NMR spectrum with different amounts of guest. The reported association constants were calculated using the software SPECFIT[24], which uses a global analysis system with expanded factor analysis and Marquardt least-squares minimization to obtain globally optimized parameters. The titration data were fitted to a simple 1 : 1 binding stoichiometry. The reported errors for the stability constants calculated by SPECFIT were estimated as the square root of the sum of the square of the standard deviation from at least three experimental values of the binding constants determined in different titration experiments.

EXSY experiments

A 2D NOESY spectrum of a solution containing the receptor hybrid cavitand **2** with an adequate molar excess of the corresponding guest ($\mathbf{1a}^+$ or $\mathbf{4}^+$) was recorded with the phase sensitive NOESY pulse sequence supplied with the Bruker software using a mixing time of 300 ms and 3 s relaxation delay between pulses. The temperature of the probe was set to 298 K during the experiment with $\mathbf{1a}^+$ and 203 K for $\mathbf{4}^+$. Each of the 512 F1 increments was the accumulation of 32 scans. Before Fourier transformation, the FIDs were multiplied by a 90° sine square function in both the F2 and F1 domain. 1 K and 1 K real data points were used in both dimensions. The integral values of the two dimensional peaks were obtained by calculating from the spectra using the Bruker processing software. The reaction rate constants k_{in} and k_{out} were derived from the exchange intensity matrix based on the integration of the cyclopentadienyl protons and using the D2DNMR software.[17]

ITC studies

ITC data were obtained on a VP-ITC MicroCalorimeter, MicroCal, LLC (Northampton, MA). The calorimetric titrations were performed by the injection of 5 μL aliquots of a solution of cobaltocenium cation **1a**$^+$, approximately seven times more concentrated than the cavitand **2a** ([**2a**] = 0.2 mM, MeOH) or **2b** ([**2b**] = 10 mM, acetone) solutions placed in the cell. After the reference titration was subtracted, the association constants and the thermodynamic parameters were obtained from the fit of the revised titration data to a theoretical titration curve using the one set of sites model of the Microcal ITC Data Analysis module provided by MicroCal, LLC. The error was taken as twice the standard error.

Electrochemical analysis

The cyclic voltammetry (CV) experiments were carried out using a EC εpsilon Electrochemica Analyzer (C3-Cell Stand). A glassy carbon disk working electrode (0.071 cm^2), a platinum wire counter electrode, and a nonaqueous Ag/AgCl reference electrode were fitted to a single-compartment cell for the voltammetric experiments. A 1.0 mM solution of the cavitand (**2a** or **2b**) was prepared containing tetraoctylammonium bromide (0.1 M) as supporting electrolyte and placed in the cell. The cobaltocenium cation **1a**$^+$ was added as a solid. The solution was deoxygenated by purging with argon gas and maintained under an inert atmosphere for the duration of each electrochemical experiment. Stirring and gas purging are available by remote control with BASI PC-controlled potentiostat. A cyclic voltammogram was recorded after each addition.

Calculation of the diffusion coefficients

The diffusion coefficients of free and included cobaltocenium cation **1a**$^+$ within cavitand **2a** were calculated by means of a series of CVs measured at different scan rates (0.025–2 V s^{-1}). We used a 1.0 mM solution of **1a**$^+$ (Fig. S12†) and an analogous solution containing 2 equivalents of **2a** (Fig. S13). In both cases, tetraoctylammonium bromide (0.1 M) was used as electrolyte and MeOH as solvent. Using the Randles–Sevcick equation ($I = (2.68 \times 10^5)\ n^{2/3}\ A\ C_{ox}\ (D_{ox}V)^{1/2}$) ($A = 0.071$ cm^2), the diffusion coefficients were calculated form the slope in the representation of I *vs.* $v^{1/2}$.[3b]

Conclusions

In conclusion, we have demonstrated spectroscopically (^{1}H NMR and ESI-MS) and voltammetrically that simple hybrid cavitand-resorcin[4]arene receptors like **2** form kinetic and thermodynamic stable inclusion complexes with cationic organometallic sandwich complexes of Co(III) complementary in size. The binding constants for cobaltocenium, **1a**$^+$, are higher than 10^3 M^{-1}. Cobalt(III) organometallic sandwich complexes having bulky ligands (Cp*) are not included within the cavity of **2**. Neutral metallocenes like ferrocene **9a**, or cobaltocene **9b** show little affinity for the electronically rich cavity of **2**. The barrier for the self-exchange of included **1a**$^+$ within receptor **2b** has been calculated as $\Delta G^{\neq 298\ K}_{diss} = 16.38$ kcal mol^{-1} using a 2D EXSY experiment. The presence of one ethyl group in both Cp rings, as in guest **4**$^+$, reduces considerably the kinetic and thermodynamic stability of the **4**$^+$@**2b** complex probably due to a shallower inclusion of the guest. However, the presence of the ethyl group reduces the rate of tumbling of the guest inside the host's cavity. In the voltammetric studies, a new redox Co(II)/Co(III) couple shifted toward cathodic values can be observed for the included **1a**$^+$. The observation of the shifted peak indicates that the cationic form of Co(III), **1a**$^+$, is more strongly bound by the hybrid cavitands **2a** and **2b** than neutral Co(II) **9b** and that the electron transfer process proceeds in the included form. The reduction of the guest eliminates the contribution of the cation–π interaction to the complex stabilities. Consequently, we have quantified this type of interaction in the complexes as 5.3 kcal mol^{-1} in the case of **2a** and 2.1 kcal mol^{-1} for **2b**. We are currently pursuing the use of these receptors for the modification of the chemical reactivity and selectivity of included metal centers.[25]

Acknowledgements

We thank Ministerio de Educación y Ciencia, SEUI, for generous grants (CTQ2005-08989-C01-C02/BQU and CSD2006–0003). We also thank ICIQ Foundation and Generalitat de Catalunya, DURSI (2005SGR00108) for financial support.

Notes and references

1 (*a*) F. Hof, S. L. Craig, C. Nuckolls and J. Rebek, Jr, *Angew. Chem., Int. Ed.*, 2002, **41**, 1488–1508; (*b*) D. Fiedler, D. H. Leung, R. G. Bergman and K. N. Raymond, *Acc. Chem. Res.*, 2005, **38**, 349–358; (*c*) M. Fujita, M. Tominaga, A. Hori and B. Therrien, *Acc. Chem. Res.*, 2005, **38**, 369–378.
2 C. M. Cardona, S. Mendoza and A. E. Kaifer, *Chem. Soc. Rev.*, 2000, **29**, 37–42.
3 (*a*) F. Hapiot, S. Tilloy and E. Monflier, *Chem. Rev.*, 2006, **106**, 767–781; (*b*) A. E. Kaifer and M. Gómez-Kaifer, *Supramolecular Electrochemistry*, Wiley-VCH, Weinheim, 1999; (*c*) W.-Y. Sun, T. Kusukawa and M. Fujita, *J. Am. Chem. Soc.*, 2002, **124**, 11570–11571; (*d*) S. Mendoza, P. D. Davidov and A. E. Kaifer, *Chem.–Eur. J.*, 1998, **4**, 864–870; (*e*) D. Ajami, M. P. Schramm, A. Volonterio and J. Rebek, Jr., *Angew. Chem., Int. Ed.*, 2007, **46**, 242–244.
4 A. E. Kaifer, *Acc. Chem. Res.*, 1999, **32**, 62–71.
5 W. Ong and A. E. Kaifer, *Organometallics*, 2003, **22**, 4181–4183.
6 L. Frish, M. O. Vysotsky, V. Boehmer and Y. Cohen, *Org. Biomol. Chem.*, 2003, **1**, 2011–2014.
7 (*a*) I. Philip and A. E. Kaifer, *J. Org. Chem.*, 2005, **70**, 1558–1564; (*b*) I. E. Philip and A. E. Kaifer, *J. Am. Chem. Soc.*, 2002, **124**, 12678–12679. Under the conditions of the electrochemical experiments described in reference 7*a*, dimeric or timeric capsules may form around the organometallic cation.
8 P. Ballester and M. A. Sarmentero, *Org. Lett.*, 2006, **8**, 3477–3480.
9 A. V. Davis, D. Fiedler, G. Seeber, A. Zahl, R. vanEldik and K. N. Raymond, *J. Am. Chem. Soc.*, 2006, **128**, 1324–1333.
10 WebLab ViewerPro 4.0, Molecular Simulations Inc..
11 D. J. Cram, K. D. Stewart, I. Goldberg and K. N. Trueblood, *J. Am. Chem. Soc.*, 1985, **107**, 2574–2575.
12 (*a*) S.-D. Tan, W.-H. Chen, A. Satake, B. Wang, Z.-L. Xu and Y. Kobuke, *Org. Biomol. Chem.*, 2004, **2**, 2719–2721; (*b*) M. Inouye, K.-I. Hashimoto and K. Isagawa, *J. Am. Chem. Soc.*, 1994, **116**, 5517–5518; (*c*) K. N. Koh, K. Araki, A. Ikeda, H. Otsuka and S. Shinkai, *J. Am. Chem. Soc.*, 1996, **118**, 755–758.
13 Non linear curve fitting afforded a similar value.
14 Examples of ITC applicability to supramolecular chemistry and host–guest recognition: (*a*) P. Ballester, A. I. Oliva, A. Costa, P. M. Deya, A. Frontera, R. M. Gomila and C. A. Hunter, *J. Am. Chem. Soc.*, 2006, **128**, 5560–5569; (*b*) V. D. Jadhav and F. P. Schmidtchen, *Org. Lett.*, 2005, **7**, 3311–3314; (*c*) J. Kerckhoffs, M. G. J. ten Cate, M. A. Mateos-Timoneda, F. W. B. van Leeuwen, B. Snellink-Ruel, A. L. Spek, H. Kooijman, M. Crego-Calama and D. N. Reinhoudt, *J. Am. Chem. Soc.*, 2005, **127**, 12697–12708; (*d*) M. G. J. ten Cate, J. Huskens,

M. Crego-Calama and D. N. Reinhoudt, *Chem.–Eur. J.*, 2004, **10**, 3632–3639; (*e*) P. Ballester, A. Costa, P. M. Deya, M. Vega, J. Morey and G. Deslongchamps, *Tetrahedron Lett.*, 1999, **40**, 171–174.
15 U. Lucking, F. C. Tucci, D. M. Rudkevich and J. Rebek, *J. Am. Chem. Soc.*, 2000, **122**, 8880–8889.
16 (*a*) M. Pons and O. Millet, *Prog. Nucl. Magn. Reson. Spectrosc.*, 2001, **38**, 267–324; (*b*) C. L. Perrin and T. J. Dwyer, *Chem. Rev.*, 1990, **90**, 935–967.
17 D2DNMR (PC version): (*a*) E. W. Abel, T. P. J. Coston, K. G. Orrell, V. Sik and D. Stephenson, *J. Magn. Reson.*, 1986, **70**, 34–53; (*b*) J. Lu, D. Ma, J. Hu, W. Tang and D. Zhu, *J. Chem. Soc., Dalton Trans.*, 1998, 2267–2274.
18 J. R. Moran, J. L. Ericson, E. Dalcanale, J. A. Bryant, C. B. Knobler and D. J. Cram, *J. Am. Chem. Soc.*, 1991, **113**, 5707–5714.
19 (*a*) D. M. Rudkevich, G. Hilmersson and J. Rebek, *J. Am. Chem. Soc.*, 1997, **119**, 9911–9912; (*b*) D. M. Rudkevich, G. Hilmersson and J. Rebek, *J. Am. Chem. Soc.*, 1998, **120**, 12216–12225.
20 T. Gottschalk, B. Jaun and F. Diederich, *Angew. Chem., Int. Ed.*, 2007, **46**, 260–264.
21 E. Menozzi, H. Onagi, A. L. Rheingold and J. Rebek, Jr., *Eur. J. Org. Chem.*, 2005, 3633–3636.
22 R. A. Zelonka and M. C. J. Baird, *J. Organomet. Chem.*, 1972, **44**, 383–389.
23 K. N. Koh, K. Araki, A. Ikeda, H. Otsuka and S. Shinkai, *J. Am. Chem. Soc.*, 1996, **118**, 755–758.
24 *SPECFIT*, v 3.0.36, Spectrum Software Associates.
25 D. Fiedler, R. G. Bergman and K. N. Raymond, *Angew. Chem., Int. Ed.*, 2006, **45**, 745–748.

